THE JOURNAL OF BIOLOGICAL CHEMISTRY VOL. 285, NO. 31, pp. 24131–24140, July 30, 2010

Target of Rapamycin (TOR)-like 1 Kinase Is Involved in the Control of Polyphosphate Levels and Acidocalcisome Maintenance in *Trypanosoma brucei*[*] [S]

Received for publication, March 5, 2010, and in revised form, May 3, 2010 Published, JBC Papers in Press, May 21, 2010, DOI 10.1074/jbc.M110.120212

Teresa Cristina Leandro de Jesus[‡§1], Renata Rosito Tonelli[‡], Sheila C. Nardelli[‡], Leonardo da Silva Augusto[‡], Maria Cristina M. Motta[¶], Wendell Girard-Dias[¶], Kildare Miranda[¶‖], Paul Ulrich[§2], Veronica Jimenez[§2], Antonio Barquilla[**], Miguel Navarro[**], Roberto Docampo[§3], and Sergio Schenkman[‡4]

*From the [‡]Departamento de Microbiologia, Imunologia e Parasitologia, Universidade Federal de São Paulo, São Paulo 04023-062, Brazil, the [§]Center for Tropical and Emerging Global Diseases and Department of Cellular Biology, University of Georgia, Athens, Georgia 30602, the [¶]Instituto de Biofísica Carlos Chagas Filho, Universidade Federal do Rio de Janeiro, Rio de Janeiro 21949-900, Brazil, the [‖]Diretoria de Programas, Instituto Nacional de Metrologia Normalização e Qualidade Industrial, Duque de Caxias, Rio de Janeiro 25250-020, Brazil, and the **Instituto de Parasitología y Biomedicina "López-Neyra," Consejo Superior de Investigaciones Científicas, Granada 18100, Spain*

Target of rapamycin (TOR) kinases are highly conserved protein kinases that integrate signals from nutrients and growth factors to coordinate cell growth and cell cycle progression. It has been previously described that two TOR kinases control cell growth in the protozoan parasite *Trypanosoma brucei*, the causative agent of African trypanosomiasis. Here we studied an unusual TOR-like protein named TbTOR-like 1 containing a PDZ domain and found exclusively in kinetoplastids. TbTOR-like 1 localizes to unique cytosolic granules. After hyperosmotic stress, the localization of the protein shifts to the cell periphery, different from other organelle markers. Ablation of TbTOR-like 1 causes a progressive inhibition of cell proliferation, producing parasites accumulating in the S/G_2 phase of the cell cycle. TbTOR-like 1 knocked down cells have an increased area occupied by acidic vacuoles, known as acidocalcisomes, and are enriched in polyphosphate and pyrophosphate. These results suggest that TbTOR-like 1 might be involved in the control of acidocalcisome and polyphosphate metabolism in *T. brucei*.

African trypanosomiasis, or sleeping sickness, is a disease caused by the parasitic protist *Trypanosoma brucei* that affects a half-million people in sub-Saharan Africa. Transmitted by the tsetse fly vector (*Glossina spp.*), trypanosomiasis represents an important public health problem and has a strong impact in the economic development of that region. *T. brucei* has a complex life cycle involving different morphological and functional stages. These parasites alternate between insect and mammalian hosts. The adaptation to these diverse environments requires rapid changes in gene expression to fulfill metabolic or morphological changes (1). This parasite also has the ability to survive a wide range of environmental conditions as it progresses through its life cycle, including extreme fluctuations in external osmolarity (2).

Target of rapamycin (TOR)[5] proteins are evolutionarily conserved protein kinases that integrate information from energy levels, mitogenic signals, and nutrient supplies regulating cell growth accordingly. Studies on mammalian cells and yeast signaling pathways have shown that nutrient starvation inhibits TOR activities, which results in G_1 cell cycle arrest, and triggers a stress response program leading to a blockade of translation initiation. Similar stress responses can be observed in cells treated with rapamycin, an immunosuppressant drug, which binds to FKBP12, a prolyl-isomerase, forming a complex with the TOR kinase (reviewed in Refs. 3 and 4).

Two distinct aspects of cell growth are regulated by two functionally different TOR kinases in *T. brucei*, termed TbTOR1 and TbTOR2. TbTOR1 and TbTOR2 function in two distinct TOR-containing multiprotein complexes (TORC) conserved along eukaryote evolution, named TORC1 and TORC2. TbTOR1, located in the nucleus, controls the synthesis and accumulation of cell mass through TORC1 signaling, whereas TbTOR2, associated with the mitochondrion or endoplasmic reticulum, controls actin cytoskeleton organization and endocytosis through TORC2 (5). Only this latter is sensitive to rapamycin, contrary to what is observed for mammalian cells and yeast, in which TORC1, but not TORC2 is sensitive to rapamy-

* This work was supported, in whole or in part, by National Institutes of Health Grant AI-077538 (to R. D.). This work was also supported by grants from Fundação de Amparo à Pesquisa do Estado de São Paulo, Fundação de Amparo à Pesquisa do Estado do Rio de Janeiro, Conselho Nacional de Desenvolvimento Científico e Tecnológico e Instituto Nacional de Ciência e Tecnologia de Vacinas do Conselho Nacional de Desenvolvimento Científico e Tecnológico, Brazil.

[S] The on-line version of this article (available at http://www.jbc.org) contains supplemental Figs. S1–S5.

[1] Supported in part by a training grant from the Ellison Medical Foundation to the Center for Tropical and Emerging Global Diseases.

[2] Supported by a postdoctoral fellowship from the American Heart Association.

[3] To whom correspondence may be addressed: Center for Tropical and Emerging Global Diseases University of Georgia, 500 D. W. Brooks Dr., Athens, GA 30602. Tel.: 706-542-8104; Fax: 706-542-9493; E-mail: rdocampo@cb.uga.edu.

[4] To whom correspondence may be addressed: Universidade Federal de São Paulo, R. Botucatu 862 8°A, 04023-062 São Paulo, SP, Brazil. Tel.: 55-11-5575-1996; Fax: 55-11-5571-5877; E-mail: sschenkman@unifesp.br.

[5] The abbreviations used are: TOR, target of rapamycin; TORC, TOR complex; PCF, *T. brucei* procyclic form(s); BSF, *T. brucei* bloodstream form(s); poly P, polyphosphate; DIC, differential interference contrast; DAPI, 4,6- diamidino-2-phenylidole; RNAi, RNA interference; PBS, phosphate-buffered saline.

cin (6). Surprisingly, two other sequences encode putative kinases with high domain similarity to TOR kinases in *T. brucei*: TbTOR-like 1 and TbTOR-like 2; one of them, TbTOR-like 1, is not found in TbRaptor- or TbAVO3-containing complexes (5). The presence of additional TOR kinases would suggest that in *T. brucei*, these enzymes could have acquired additional roles to those carried out for TORC1 or TORC2, possibly related to their adaptation to different hosts and environments.

In this work we investigated the role of TOR-like 1 protein in *T. brucei*. Among Eukarya TOR kinases, TbTOR-like 1 possesses a unique PDZ domain, which is thought to be involved in protein-protein interactions, mediating binding of a class of submembranous proteins to membrane receptors and ion channels (7). We show that RNAi knockdown produces cells with enlarged acidocalcisomes rich in pyrophosphate (PPi) and polyphosphate (poly P), which is a polymer of a few to hundreds of phosphate units bound by phosphoanhydride bonds (8). Acidocalcisomes are organelles known to accumulate poly P in *T. brucei* as well as most protists (9). Poly P is known to regulate the activity of mammalian TOR (10) and is important for cellular adaptation to different stresses (11). Acidocalcisomes were first characterized in *T. brucei* (12) and *Trypanosoma cruzi* (13) and are electron-dense membrane-bounded vesicles rich in calcium, sodium, zinc, and magnesium, in addition to PP_i and poly P. These components and several membrane pumps and cation exchangers present in the membrane of acidocalcisomes (14–17) are implicated in the control of cell size in response to different osmotic stresses. We provide evidence that TbTOR-like 1 is implicated in the osmotic responses through control of poly P levels and acidocalcisome size.

EXPERIMENTAL PROCEDURES

Trypanosome Cultures and Transfections—The procyclic forms (PCF) of *T. brucei* strains 427 and 29-13 (18) were maintained at 27–28 °C in SDM-79 medium supplemented with 10% fetal bovine serum. For the 29-13 strain 50 μg/ml hygromycin and 15 μg/ml G418 were added to the culture medium to preserve the integrated copies of T7 RNA polymerase and the tetracycline repressor, respectively. The bloodstream forms (BSF) of *T. brucei* 90-13 (19) were cultured at 37 °C at 5% CO_2 in HMI-9 medium supplemented with 10% fetal bovine serum and 10% Serum Plus (SAFC Biosciences™) in the presence of hygromycin (5 μg/ml) and G418 (2.5 μg/ml). Cell densities were determined using a Neubauer chamber, and growth curves were performed using duplicate cultures, diluted to 1×10^6 cells/ml (PCF) or to 1×10^5 cells/ml (BSF) to begin the experiment.

RNAi Experiments—For RNAi, a 457-nucleotide fragment of TbTOR-like 1 (nucleotides 430–886) of the sequence deposited in the GenBank™ as XM_839137 was amplified by PCR using primers 5′-CGGATCCCTTCTTGGGAAGCATTTTGG and 5′-AAGCTTTATACCCTCCAGTCACG. This sequence encodes a portion of the TbTOR like 1 gene, coding fragment 1. For TbTOR2 RNAi, a 436-nucleotide fragment (nucleotides 85–520) from the sequence deposited in the GenBank™ as XM_839099, we used the primers 5′-GGGATCCGCTGAGGTTGTTAAGCAGGC and 5′-AAGCTTACATGTCGAGAATTCGC. Both pairs of primers incorporated BamHI and HindIII sites (underlined nucleotides, respectively) sites at opposite ends of the DNA fragments. Fragments were cloned into pCR 2.1 TOPO (Invitrogen) and subcloned into the BamHI and HindIII sites of the p2T2-177 vector (20). The plasmids were linearized with NotI and introduced into PCF 29-13 and BSF 90-13 by electroporation. Log phase PCF (2.5×10^7) or BSF (1×10^7) were washed with Cytomix buffer (21) and electroporated with two pulses in the presence of 10 μg of purified plasmids in a 4-mm cuvette at 1.5-kV voltage and 25-microfarad capacitance. After a 24-h recovery in medium, the cells were selected with the addition of 2.5 μg/ml phleomycin. After selection, the induction of double-stranded RNA was obtained by adding 1 μg of fresh tetracycline/ml of culture every time the cells were diluted.

Antibodies—Antibodies against Tb TOR-like 1 (fragment 2) were generated by immunizing mice with a recombinant protein expressed in pET 14b containing a 513-bp fragment that was amplified by PCR using the primers 5′-CTCGAGTCTGGTGGCGACGAGGCTG and 5′-AAGCTTAACTTCCCCCCCTTGTCGGAG. The recombinant protein was obtained in inclusion bodies and purified by chromatography on nickel chelating resin in the presence of 6 M urea followed by preparative SDS-PAGE. Fragment 3 antibodies were obtained as described (5).

Preparation of Whole Cell Extracts and Western Blot Analysis—PCF and BSF were harvested by centrifugation (1,500 × *g* for 10 min), washed twice in PBS, and resuspended in PBS with 1% SDS and proteinase inhibitors (2 mM benzamidine, 1 μg of leupeptin/ml, 4 μg of aprotinin/ml, 10 μg of pepstatin A/ml, 1 μg of antipain/ml, 1 mM phenylmethylsulfonyl fluoride, 10 mM sodium pyrophosphate, 1 mM NaF) and broken with three cycles of freezing and thawing. The samples were quantified using the BCA protein kit (Pierce), mixed with 2× SDS-PAGE loading buffer, and boiled for 5 min. The cell lysates were resolved by SDS-PAGE, and the proteins were transferred onto nitrocellulose membranes (Bio-Rad) using a Bio-Rad transblot apparatus (Bio-Rad) in 500 mM Tris, 1 M glycine, 0.1% SDS buffer, pH 8, containing 10% methanol. Nonspecific binding was blocked with 5% nonfat milk in PBS-T (PBS containing 0.1% Tween 20) for 1 h at room temperature. The antibodies were also diluted in PBS-T containing 5% nonfat milk. The membranes were incubated with anti-TbTOR-like 1 fragments 2 and 3 at a dilution of 1:300 overnight at 4 °C or with anti-α-tubulin monoclonal antibody (Sigma) at a dilution of 1:15,000. After three washes of 10 min with PBS-T, the membranes were incubated with horseradish peroxidase-conjugated goat anti-rabbit IgG or anti-mouse IgG (Sigma) diluted at 1:15,000 and 1:10,000, respectively, for 1 h. After three washes of 10 min each with PBS-T, bound antibodies were detected using a chemiluminescence kit (Pierce) according to the manufacturer's instructions.

Northern Blot Analysis—Total RNA was purified from 2×10^8 cells using TRIzol reagent (Invitrogen) according to the manufacturer's protocol. Samples of RNA (20 μg) were separated on a 1% formaldehyde-agarose gel (22), and the gel was stained with ethidium bromide. The RNA was transferred onto a Hybond NX nylon membrane (GE Healthcare) by capillary transfer and fixed by UV irradiation. The membranes were pre-

hybridized and hybridized as described in Ref. 23 with probes labeled using the Rediprime II random prime labeling system (GE Healthcare) in the presence of 50 μCi of [α-^{32}P]dCTP (3000 Ci/mmol; New England Nuclear). The tubulin probe used was a fragment of the gene cloned in the pZJM vector (24). The membranes were exposed on a phosphorimaging screen for 24 h, and labeling was detected using a Typhoon 9200 image scanner (GE Healthcare).

Fluorescence Experiments—For immunofluorescence, the cells were harvested by centrifugation at 1,500 × g for 10 min, washed with PBS two times, fixed with 2% *p*-formaldehyde in ice-cold PBS for 20 min, and settled onto poly-L-lysine-coated slides for 15 min. The fixed cells were then washed three times with PBS and permeabilized with 0.3% Triton X-100 in PBS for 3 min, washed again with PBS three times, and blocked with PBS with 3% bovine serum albumin for 1 h at room temperature. The cells were incubated with mouse anti-TbTOR-like 1 F2 (1:600 dilution), rabbit anti-HSP70 or anti-BiP (both of them gifts from James D. Bangs, University of Wisconsin-Madison Medical School (25, 26)) (1:5,000), rabbit anti-aldolase (a gift from Paul A. M. Michels, Université Catholique de Louvain, Belgium) (1:4,000 dilution), rabbit anti-Dhh1 (a gift from Dr. Samuel Goldenberg, Instituto Carlos Chagas-Fiocruz, Brazil (27)) (1:100), rabbit anti-TbVP1 (28) (1:1,000), or rabbit anti-dihydrolipoamide dehydrogenase (provided by Kevin M. Tyler, University of East Anglia, UK (29)) (1:1,000), all diluted in PBS with 3% bovine serum albumin for 1 h at room temperature. After three washes with PBS, the cells were incubated with Alexa-Fluor 546 or 488 conjugated either to goat anti-mouse IgG or Alexa-Fluor 594-conjugated goat anti-rabbit IgG (Invitrogen) at a dilution of 1:1,000 for 40 min. The cells were washed and counterstained with 1 μM 4,6-diamidino-2-phenylidole (DAPI) before mounting with Vectashield anti-fading medium (Vector Laboratories). The cells were visualized with an Olympus IX-71 inverted fluorescence microscope. Serial images (0.2 μm) were acquired with a Photometrix CoolSnapHQ charge-coupled device camera driven by DeltaVision software (Applied Precision). Alternatively, serial images (0.2-μm Z-increment) were collected using a 100× objective 1.40 NA using the Cell^M software (Olympus Europe) in a motorized Olympus IBX81 microscope. The images were processed by blind deconvolution using Autoquant X 2.1.

For observation of acridine orange accumulation, the cells were prepared as described in Ref. 28. After incubation with 6 μM of acridine orange in a buffer containing 116 mM NaCl, 5.4 mM KCl, 0.8 mM $MgSO_4$, 5.5 mM glucose, 50 mM K-HEPES, pH 7.2 (buffer A), for 10 min at 28 °C, the cells were centrifuged at 2,000 × *g*, resuspended in PBS, adhered to coverslips pretreated with 0.1% poly-L-lysine, and observed on an Olympus IX-71 inverted fluorescence microscope.

Cell Cycle Analysis—Cell samples for flow cytometry analysis were prepared as described previously (30). The cells were analyzed with a FACSCalibur using CellQuest software (Becton Dickinson). For image analysis, the cells were fixed, adhered, and permeabilized as described above, stained with 10 μg/ml of DAPI for 10 min, and visualized with a fluorescence microscope.

Osmotic Stress under Constant Ionic Conditions—For osmotic stress under constant ionic strength, the following buffers described previously (31) were used: isotonic (64 mM NaCl, 4 mM KCl, 1.8 mM $CaCl_2$, 0.53 mM $MgCl_2$, 5.5 mM glucose, 5 mM Na-HEPES, pH 7.4, and 150 mM mannitol; 282 mOsm/liter), hypotonic (the same as isotonic but with reduced mannitol concentration to 50 mM; 177 mOsm/liter), and hypertonic (the same as isotonic but with increased mannitol concentration to 500 mM; 650 mOsm/liter). Samples of 2 × 10^7 cells were collected, washed twice with PBS, and resuspended in 10 ml of isosmotic buffer. To the resuspended cells 500 μl of the desired buffer (isosmotic, hyposmotic or hyperosmotic) were added, and the samples were fixed with an equal volume of 8% paraformaldehyde in PBS after the indicated periods of time. The cells were collected by centrifugation, washed once with PBS, and adhered to coverslips pretreated with 0.1% poly-L-lysine for 1 h and processed for immunofluorescence as described above.

Electron Microscopy—For thin section images, trypanosomes were collected and fixed with 2.5% glutaraldehyde, 4% freshly prepared paraformaldehyde, and 0.1 M sodium cacodylate buffer, pH 7.3, on ice for 1 h and processed as described (32). The images were obtained in a Zeiss EM 902 microscope. For imaging whole cells, PCF were washed twice with filtered buffer A and directly applied to Formvar-coated grids as described previously (33). The images were observed in an energy-filtering Zeiss EM 902 microscope. The number of acidocalcisomes was obtained as in Ref. 33.

Quantification of PP_i, Long Chain, and Short Chain poly P—PP_i and poly P were extracted from 2.5 × 10^7 PCF and 1 × 10^8 BSF collected by centrifugation and washed three times with buffer A (described above). For short chain poly P and PP_i extraction, the cell pellet was resuspended in 100 μl of buffer A and 200 μl of ice-cold 0.5 M perchloric acid and left on ice for 30 min. The suspension was centrifuged at 10,000 × *g* for 1 min, and the supernatant was neutralized by the addition of 0.72 M KOH, 0.6 M $KHCO_3$. Precipitated $KClO_4$ was removed by centrifugation at 10,000 × *g* for 1 min, and the supernatant was used for measuring the phosphorus and PP_i released. Long chain poly P was extracted as described in Ref. 33.

Enzymatic assays of poly P and PP_i were performed in triplicate. The assays for short chain poly P were incubated at 35 °C for 30 min in 20 mM Tris-HCl, pH 7.5, 100 mM ammonium acetate, 5 mM magnesium acetate containing the sample, and >50 units of yeast exopolyphosphatase (34). Background phosphate contamination of each sample was measured in triplicate wells not containing the exopolyphosphatase, and positive control reactions were included on each plate containing a final concentration of 20 μM sodium triphosphate. The reactions were stopped by the addition of freshly mixed, malachite green reagent (3 parts 0.045% malachite green and 1 part 4.2% ammonium molybdate, 4 M HCl), and absorbance at 660 nm was immediately read on a M2e microplate spectrophotomer (Molecular Devices). Release of phosphate from PP_i was performed for 10 min at 35 °C in 50 mM Tris, pH 7.5, containing 5 mM $MgCl_2$ and 0.1 unit of yeast pyrophosphatase (Sigma). Background phosphate controls (no pyrophosphatase) and positive control (20–25 μM potassium pyrophosphate) wells

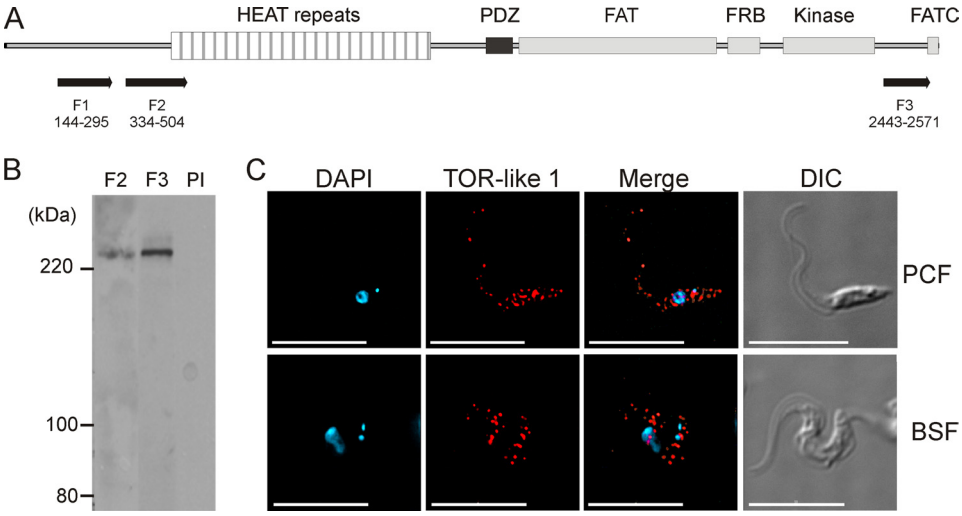

FIGURE 1. **Identification and localization of TbTOR-like kinase in PCF and BSF of *T. brucei*.** *A*, schematic representation of TbTOR-like 1 and its structural domains. The portion used for RNAi (*F1*) and those used for antibody generation (*F2* and *F3*) are indicated. *B*, immunoblot analysis of whole cell extracts of PCF (strain 29-13) with antibodies generated against TbTOR-like 1 (*F2* and *F3*) and a preimmune serum (*PI*). The molecular mass markers are indicated on the *left*. *C*, immunofluorescence analysis showing localization of TbTOR-like 1 in 29-13 PCF and 90-13 BSF with anti-TbTOR-like antibodies (F2, in *red*). The figure also shows DAPI staining (*blue*), the merged fluorescence images, and DIC images of the same field. *Scale bars*, 10 μm.

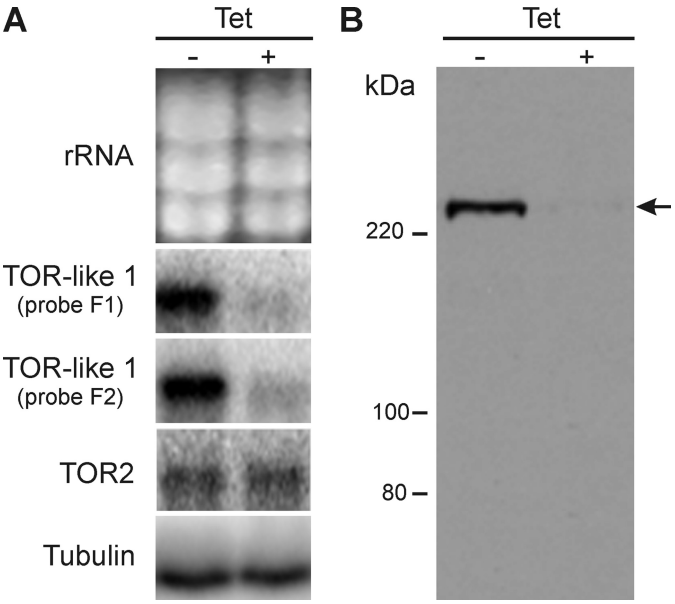

FIGURE 2. ***T. brucei* shows decreased mRNA and protein levels of TbTOR-like 1 after ablation by RNAi.** *A*, Northern blot analysis of PCF (29-13) containing an integrated copy of the RNAi construct p2T7-177 TbTOR-like 1. RNAi was induced by the addition of 1 μg/ml of tetracycline for 7 days. Total RNA of RNAi-induced cells (+*Tet*) and noninduced cells (−*Tet*) were extracted, separated in formaldehyde-agarose gel, and analyzed by Northern blot. 20 μg of protein were loaded per lane, and the gel was stained with ethidium bromide to quantify the ribosomal RNA (*rRNA*). Blotted nylon membranes were then hybridized with two different probes (*F1* or *F2*) of TbTOR-like 1 or with a tubulin probe as a loading control. *B*, immunoblot analysis after RNAi of TbTOR-like 1. Untreated (−*Tet*) and tetracycline-treated (1 μg/ml) (+*Tet*) PCF containing the integrated p2T7-177 TbTOR-like 1 vector were collected after 6 days and processed for immunoblot analysis using anti-TbTOR-like 1 antibody (*F2*). The molecular mass markers are shown on the *left*.

were included in triplicate. Phosphate was measured with malachite green as described above. On all occasions, standard curves of potassium phosphate were included on each plate. Both phosphate content released from poly P and pyrophosphate were normalized to reaction yield as determined by positive controls. Calculations of concentrations of short and long chain poly P and PP_i were based in the number of cells used in the extraction (amount of P_i or $PP_i/10^6$ cells).

RESULTS

TbTOR-like 1 Sequence Contains an Unusual PDZ Domain—The *T. brucei* genome data base contains sequences for four open reading frames encoding for proteins with sequences similar to mammalian TOR: TbTOR1, TbTOR2, TbTOR-like 1, and TbTOR-like 2. TbTOR1 and TbTOR2 proteins were previously described by Barquilla *et al.* (5). The TbTOR-like 1 gene is located in chromosome 4 and has 7788 base pairs in length encoding for a 291.11-kDa protein with an isoelectric point of 5.92. The predicted protein contains the conserved sequence domains found in TbTOR1/2, ScTbTOR1/2, and mTOR: HEAT repeats (repeats of an amino acid sequence motif that was first identified in Huntingtin, in elongation factor 3, in the regulatory subunit of Protein Phosphatase 2A, and in the TOR, which function in transport processes) (35), the FAT domain (found in FRAP, ATM, and TRRAP proteins involved in protein-protein interactions) (36), the FKBP12-rapamycin binding domain (37), the kinase domain (catalytic domain with homology to phosphatidylinositol kinases), and the FATC domain (found at the extreme carboxyl terminus, always in combination with the FAT domain (36) (Fig. 1*A*). The main difference between the TbTOR-like 1 domain structure and the canonical structure of the TOR kinases is the presence of a PDZ domain (38) between the HEAT repeats and the FAT domain.

Subcellular Localization of TbTOR-like 1—PDZ domains are usually present in proteins that interact marginally with membranes. Thus, we investigated the subcellular localization of TbTOR-like 1. In immunoblots anti-F2 and -F3 antibodies reacted with a band of 291 kDa, the expected size for TbTOR-like 1 (Fig. 1*B*). Immunofluorescence using anti-F2 antibodies revealed a granular pattern, which is distributed through the cytosol in PCF and BSF (Fig. 1*C*). To initially confirm the cellular localization of TbTOR-like 1, RNAi experiments were made in procyclic forms using a vector that generates double strand RNA from a single construct containing the gene segment corresponding to F1. Northern blot analysis shows that RNAi specifically ablated the expression of TbTOR-like 1 (Fig. 2*A*). Similarly, the levels of protein recognized by immunoblots using anti-F2 or F3 antisera against TbTOR-like 1 decreased. Fig. 2*B* shows the results for anti-F2, but identical decreases were observed when using anti-F3 antibodies. Knockdown of TbTOR-like 1 is already observed 24 h after RNAi induction with tetracycline, without an immediate effect in cell growth for PCF (Fig. 3*A*) or BSF (Fig. 3*B*). Importantly, the immunofluorescence analysis showed a convincing decrease in labeling in

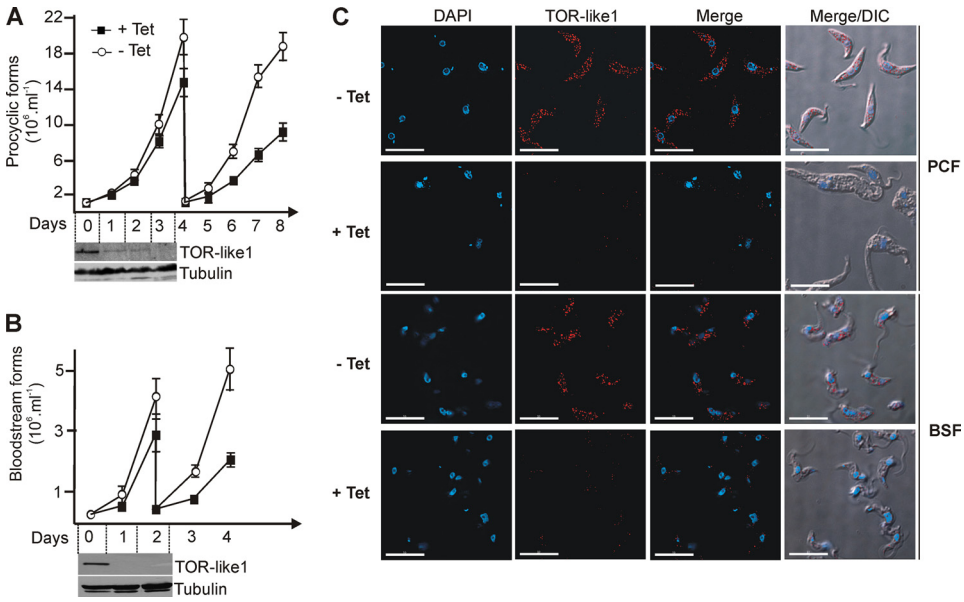

FIGURE 3. **TbTOR-like 1 ablation by RNAi causes a progressive cell growth inhibition in PCF and BSF of *T. brucei*.** *A* and *B*, growth curve of tetracycline induced (+*Tet*) or noninduced (−*Tet*) PCF (*A*) and BSF (*B*). At days 4 and 3 the cells were diluted again to the initial dilution (1×10^6/ml and 3×10^5/ml for PCF and BSF, respectively). The values are the means ± S.D. of triplicate experiments. The differences were statistically significant for PCF at days 6, 7, and 8 ($p = 0.011$, 0.003, and 0.025, respectively) and for BSF at days 3 and 4 ($p = 0.023$ and 0.038, respectively). *Lower panels*, immunoblot of whole cell extracts of the same cells treated with tetracycline collected at the indicated days and revealed with anti-TbTOR-like 1 (F2) or with anti-tubulin antibodies as a loading control. *C*, immunofluorescence analysis of PCF and BSF TbTOR-like 1 RNAi cell lines, induced (+*Tet*) or not (−*Tet*) with tetracycline and using anti-TbTOR-like 1 (F2, *red*). The figure also shows DAPI staining (*blue*) and the merged fluorescence images of the same field. Corresponding DIC images are shown as well. *Scale bars*, 10 μm.

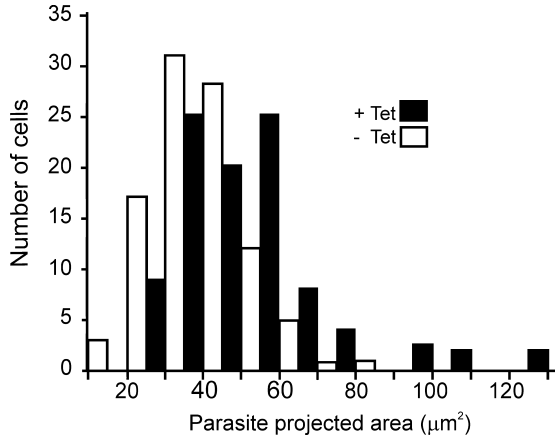

FIGURE 4. **TbTOR-like 1 ablation causes an increase in cell size.** PCF were induced (+*Tet*, *black bars*) or not (−*Tet*, *white bars*) with tetracycline for 4 days, fixed, and adhered to coverslips as described under "Experimental Procedures," and the images were taken using DIC. Binaries were generated using the ImageJ software, and the area of each cell image was quantified. The graph shows the distribution of *T. brucei* projected surface area. The two distributions were statistically different ($p < 0.05$) based on a nonparametric Student's *t* test ($n = 98$ and 100 for noninduced and induced RNAi, respectively). No significance difference was observed for PCF 29-13 in the presence compared with the absence of tetracycline.

both PCF and BSF (Fig. 3*C*), confirming the cellular localization of TbTOR-like 1.

We found that TbTOR-like 1 is in the cytosol and is not associated with major organelles. Its labeling pattern shows some colocalization with anti-HSP70 (a cytosolic marker) but differs significantly with respect of anti-aldolase (a glycosomal marker), anti-Dhh1 (a P-body marker), anti-TbVP1 (an acidocalcisome marker), anti-dihydrolipoamide dehydrogenase (a mitochondrial marker), and anti-BiP (an endoplasmic reticulum marker) localization (supplemental Fig. S1). Cell fractionation studies revealed that, different from TbTOR2, which is associated with the parasite mitochondria or with the endoplasmic reticulum (5), TbTOR-like 1 is found in the soluble fraction and not associated with membranous cell compartments (supplemental Fig. S2).

Phenotypic Analysis of TbTOR-like 1 RNAi Cell Line—It can be noted from Fig. 3 (*A* and *B*) that RNAi of TbTOR-like 1 progressively decreased cellular proliferation, whereas protein expression disappears rapidly in PCF and BSF. The effect of proliferation is more pronounced several days following knockdown. In addition, TbTOR-like 1-depleted PCF (but not BSF) appear larger than the noninduced controls (Fig. 3*C*, *DIC*). Morphometric analysis of a large number of cells confirmed this observation. The projected area taken from two-dimensional images revealed that RNAi-induced cells were larger than the noninduced controls (Fig. 4).

TbTOR-like 1-depleted PCF Are Arrested in the S/G_2 Phase of the Cell Cycle—The increased size of cells lacking TbTOR-like 1 could be due to a delayed progression in the cell cycle, which would also explain the decrease in the proliferation rate. Therefore, the cellular DNA content/cell was quantified by flow cytometry after propidium iodide staining, 4 days after RNAi induction with tetracycline. As shown in Fig. 5*A*, the number of PCF in the G_1 phase of the cell cycle was reduced concomitantly with an increase of cells in the S phase. No effect of tetracycline was observed in control cells (29-13 procyclics) as shown in Fig. 5*B*. We also quantified the number of cells containing one nucleus and one kinetoplast (1N1K), 1N2K, and 2N2K and abnormal cells (0N1K) in the population using DAPI staining. Cells with one nucleus and an elongated kinetoplast corresponding to cells in the S phase were also counted as 1N2K. A decrease in 1N1K cells was found with an increased number of other patterns when comparing depleted TbTOR-like 1 cells with control cells, confirming the cell cycle delay with an increase in S/G_2 (1N2K) cells observed by fluorescence-activated cell sorter analysis (Fig. 5*C*).

Ablation of TbTOR-like 1 Increases the Size of Acidocalcisomes in Electron Microscopy Images—RNAi-induced and noninduced populations of PCF were fixed and processed for transmission electron microscopy. As shown in Fig. 6*A*, knocked down cells had an apparently higher number of electron-dense vesicles when compared with control cells.

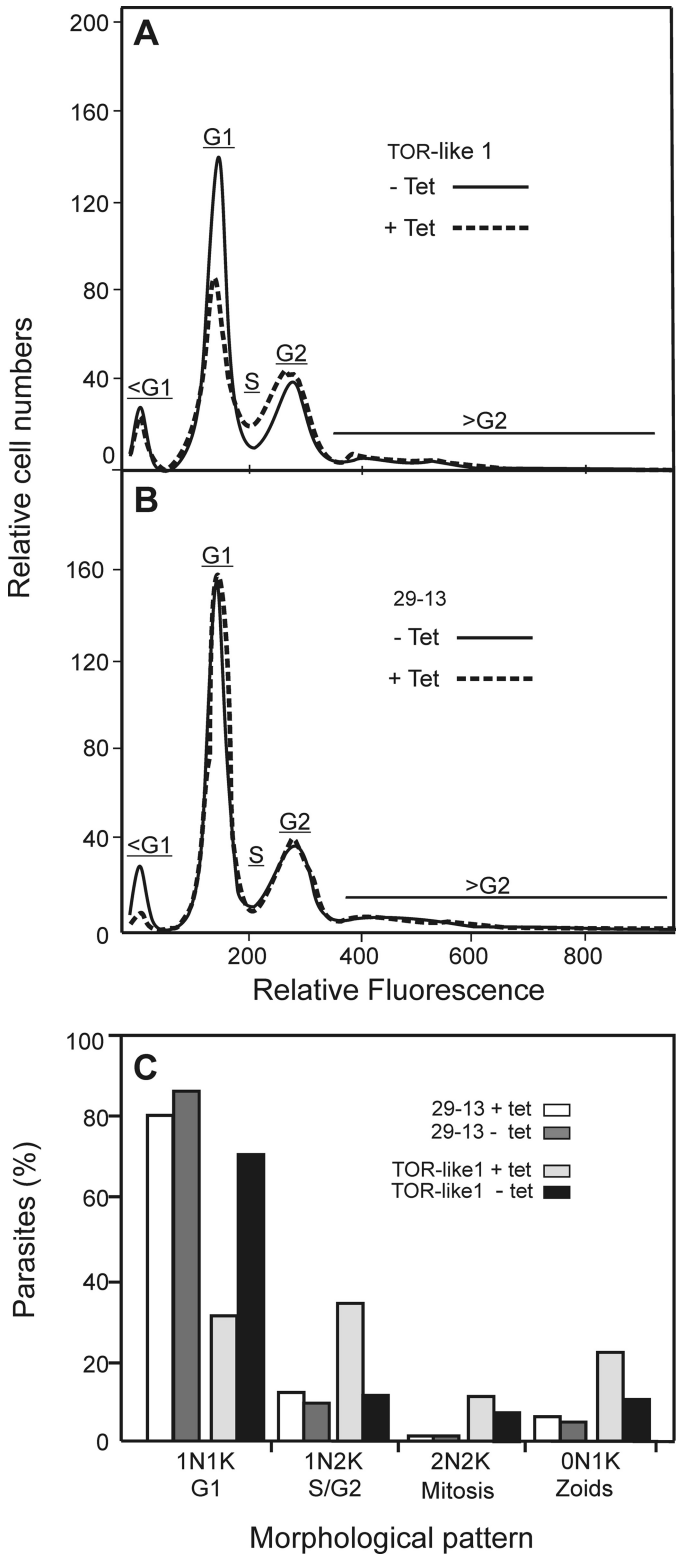

FIGURE 5. **A decrease expression of TbTOR-like 1 causes a partial arrest of the cell cycle in S/G_2.** *A* and *B*, after 4 days, untreated (−*Tet*) and 1 μg/ml tetracycline-treated (+*Tet*) PCF of TbTOR-like 1 RNAi cell line (*A*) or control 29-13 cells (*B*) were stained with propidium iodide and subjected to fluorescence-activated cell sorter analysis for DNA content or fixed and processed for DAPI staining and microscopic observation under a fluorescence microscope. *C*, number of cells ($n = 200$ for each control or TbTOR-like 1 RNAi cell line, induced or noninduced, as indicated) with different numbers of nuclei (*N*) and kinetoplasts (*K*). The differences between induced and noninduced TbTOR-like 1 were statistically different for G_1 ($p = 0.003$), G_2 ($p = 0.0023$), and zoids ($p = 0.012$). The other differences were not statistically significant.

These electron-dense vesicles appear to correspond to acidocalcisomes, which appear in conventional electron microscopy as electron-dense or partially empty vesicles (32). In normal cells the electron density corresponds to cations associated with PP_i and poly P, and these components are lost during the conventional processing for transmission electron microscopy (9, 32). Indeed, more stained acidocalcisomes were detected in TbTOR-like 1-depleted PCF when compared with control cells fixed and analyzed by energy-filtering transmission electron microscopy (Fig. 6*B*), a suitable method to observe acidocalcisomes (32). Quantitative analysis indicated that although the number of acidocalcisomes did not increase significantly when the total population of cells was analyzed, the volume and area occupied by acidocalcisomes increased significantly (Table 1). RNAi of TbTOR-like 1 also promoted a larger accumulation of acridine orange, a weak base that is incorporated into acidic compartments, such as the acidocalcisomes (Fig. 6*C*).

Ablation of TbTOR-like 1 Increases Polyphosphate and Pyrophosphate Levels—Taking into account that knockdown of TbTOR-like 1 seems to increase the size of acidocalcisomes, we determined the levels of short and long chain poly P and PP_i. As shown in Fig. 7 (*A* and *C*), the knockdown cells (PCF and BSF) contained higher levels of both types of poly P when compared with control (noninduced) cells, although the increase in short chain poly P was more evident than that of long chain poly P. The levels of PP_i also increased significantly when RNAi was induced (Fig. 7, *B* and *D*). In contrast to these results, RNAi of TbTOR2 did not significantly affect the levels of short chain poly P (supplemental Fig. S3), as compared with control (noninduced) cells. Previous transmission electron microscopy data did not reveal the presence of more electron-dense vesicles in TbTOR2 or TbTOR1 knockdowns (5). These results indicate that acidocalcisome size and poly P levels are specifically increased in cells lacking TbTOR-like 1 kinase.

Localization of TbTOR-like 1 Change after Hyperosmotic Stress—Acidocalcisomes are organelles involved in osmoregulation (9, 39). Therefore, the increase in acidocalcisomes and poly P levels in cells having less TbTOR-like 1 could therefore suggest that this kinase participates in a signaling cascade affecting acidocalcisome function. To obtain some insight about a possible mechanism of signaling activation by TbTOR-like 1, we subjected PCF (strain 29-13) to hyposmotic and hyperosmotic shocks under constant ionic conditions. Subsequently the cells were fixed and processed for immunofluorescence with anti-TbTOR-like 1 antibody. Upon hyposmotic shock the cells rapidly swell and then recover. Upon hyperosmotic stress, cells rapidly shrink and then recover their volume. These processes occur in less than 5 min. As shown in Fig. 8, only under hyperosmotic conditions do TbTOR-like 1 granules have a distinct distribution, becoming localized aligned at the cell periphery, whereas the localization of TbTOR-like 1 remains spread through all the cytosol in control or hyposmotic conditions. The relocalization pattern of TbTOR-like 1 was not observed for aldolase, a glycosome marker (supplemental Fig. S4*A*), and BiP, an endoplasmic reticulum marker (supplemental Fig. S4*B*). A partial relocalization to the surface was

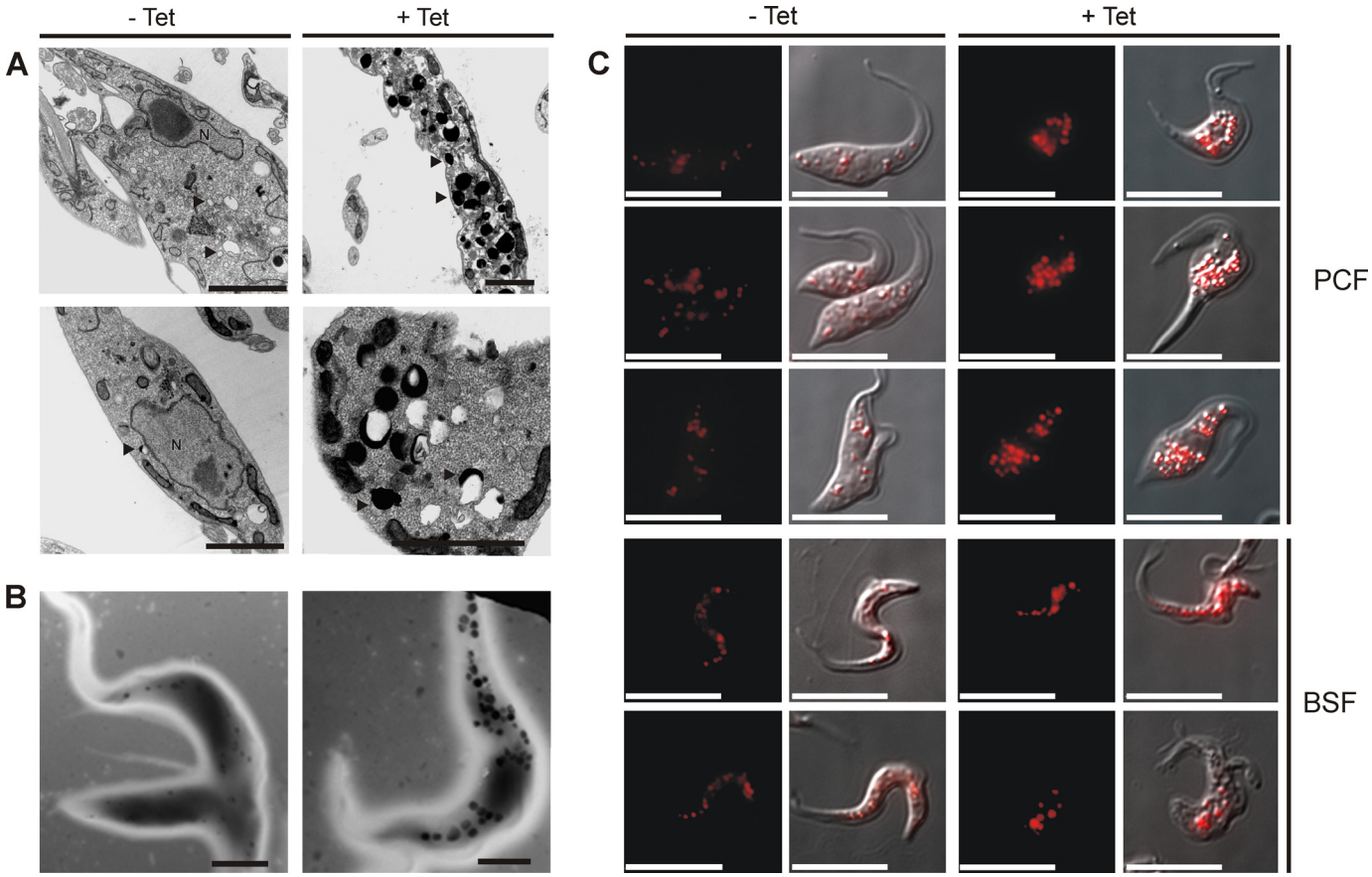

FIGURE 6. **TbTOR-like RNAi cell line presents acidocalcisomes with increased size.** *A*, transmission electron microscopy images of thin sections of resin-embedded PCF previously induced (+*Tet*) or not (−*Tet*) for 4 days with tetracycline. The *arrowheads* indicate some acidocalcisomes. *N*, nucleus. *B*, transmission electron microscopy of whole PCF attached to Formvar grids after 4 days of treatment without or with tetracycline. In both *A* and *B* the dark granules are acidocalcisomes. *Scale bars*, 2 μm in *A* and *B*. *C*, fluorescence images showing the accumulation of acridine orange in RNAi for TbTOR-like 1 cells (+*Tet*) compared with noninduced cells (−*Tet*). The *three top rows* correspond to PCF, and the *bottom two rows* correspond to BSF. *Red* pseudo color was generated using Adobe Photoshop. *Scale bars*, 10 μm.

TABLE 1

Morphometric analysis of the acidocalcisomes in *T. brucei* TOR-like 1 mutants

The results are expressed as the means ± S.D. ($n = 100$). The mean area, mean diameter, and mean volume differences have significant differences according to Student's *t* test ($p < 0.05$).

	Number of acidocalcisomes/cell	Mean area	Mean circularity	Mean diameter	Mean volume
		nm^2	*nm*	*nm*	nm^3
Without tetracycline	26 ± 8	$58.0 \pm 35.5 \times 10^3$	0.92 ± 0.03	286.2 ± 76.6	$20.4 \pm 10.4 \times 10^6$
With tetracycline	31 ± 9	$162.0 \pm 74.0 \times 10^3$	0.90 ± 0.01	477.4 ± 106.3	$81.2 \pm 57.5 \times 10^6$

observed for the dihydrolipoamide dehydrogenase mitochondrial marker (supplemental Fig. S4*C*).

A possible link between the hyperosmotic stress and polyphosphate was proposed earlier based on a previous observation that adding hyperosmotic solution to *T. cruzi* increased the levels of poly P (11). We found that cultivating *T. brucei* in medium supplemented with 0.3 M mannitol reduced growth and also increased poly P levels (Fig. 9*A* and *B*). Importantly, upon RNAi induction for TbTOR-like 1, poly P starts to increase soon after induction, before growth arrest (Fig. 9, *C* and *D*). As shown before for *T. cruzi*, poly P is high in the lag phase and decreases when the cells grow exponentially.

These results would suggest that cells lacking TbTOR-like 1 would be more sensitive when growing at higher osmolarity. Indeed, this seems to be the case. In the presence of mannitol, the effect of knocking down TbTOR-like 1 occurs earlier than in regular medium (supplemental Fig. S5). These results suggest that TbTOR-like 1 kinase participates in the control of osmotic stress response as a consequence of changes in the poly P and acidocalcisomes.

DISCUSSION

In this is study we characterized a novel type of TOR-like protein present in *T. brucei* and not previously found in any other Eukarya. Ablation of this TbTOR-like by RNAi leads to a progressive inhibition of cell proliferation, with increases in the size of acidocalcisomes and in the content of poly P and PP_i. This protein kinase is found in cytosolic granules dispersed through the cytosol, which specifically relocalizes toward the cell periphery under hyperosmotic conditions. Hyperosmotic

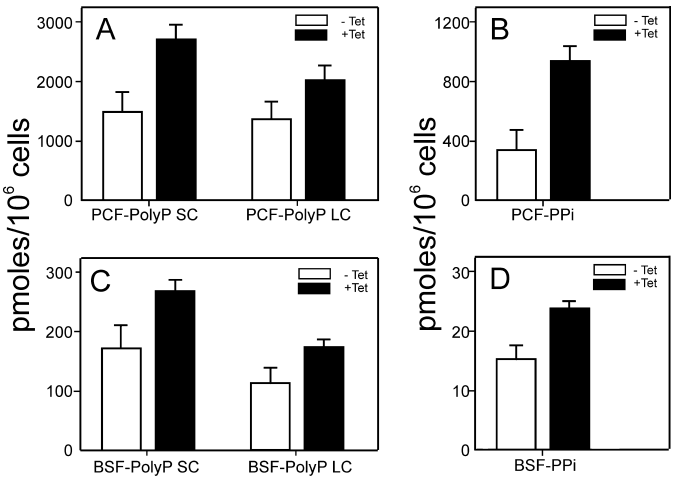

FIGURE 7. **TbTOR-like 1 ablated cells have higher levels of poly P and PP_i.** The levels of short chain (*SC*) and long chain (*LC*) poly P and the levels of PP_i were measured in noninduced (−*Tet*) and induced (+*Tet*) PCF (*A* and *B*) or BSF (*C* and *D*) after 6 and 4 days with tetracycline, respectively. The figure shows the mean values ± S.D. of three experiments measured in triplicate. The differences between noninduced and induced cells were found significant by using Student's *t* test ($p < 0.005$).

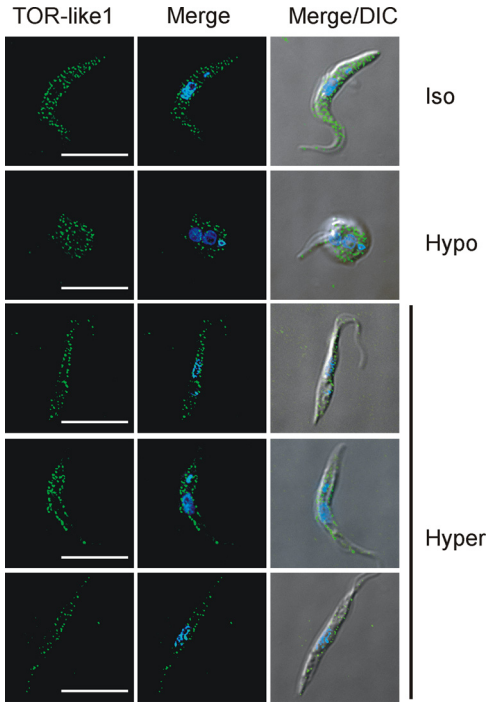

FIGURE 8. **TbTOR-like 1 relocalizes to the cell periphery in PCF submitted to hyperosmotic conditions.** *T. brucei* PCF (29-13) at exponential growth were collected by centrifugation and resuspended with isosmotic (*Iso*), hyposmotic (*Hypo*), and hyperosmotic (*Hyper*) buffers as described under "Experimental Procedures." Ten seconds after different buffer treatments, the cells were fixed and processed for immunofluorescence with anti-TbTOR-like 1 (F2) antibody (*green*) in the presence of DAPI (*blue*). The merged fluorescence images and the merged fluorescence and DIC images are shown as well. *Scale bars*, 10 μm.

conditions increase poly P levels, arrest cell growth, and sensitize parasites to TOR-like 1 dependence. These results suggest a link between TOR-like kinase 1 signaling pathway and cell responses to osmotic stresses.

TbTOR-like 1 is expressed as a cytosolic 291-kDa protein in BSF and PCF of *T. brucei* and in both forms is required for normal cell growth. The absence of this protein kinase seems to affect proliferation after several rounds of cell division, suggesting that the growth defect is due to a cumulative effect. A parallel accumulation of poly P and PP_i inside acidocalcisomes, which increase in size and become heavily stained at the electron microscopy level, is observed when compared with control cells. Cellular proteins remain at the same level as judged by quantitative profiles of two-dimensional gel electrophoresis (data not shown).

It is possible that the accumulation of poly P in acidocalcisomes is a consequence of the growth arrest determined by TbTOR-like 1 knockdown. In this regard, conditions that favor growth arrest, such as hyperosmotic stress, also result in increased poly P synthesis and in potentiation of the effects of TbTOR-like 1 knockdown (Fig. 9). The mechanism, by which the absence of TbTOR-like 1 leads to an increased content of poly P, is presently unknown, but it could be due to a direct effect on enzymes affecting the turnover of poly P, as occurs in bacteria submitted to amino acid starvation (40). Amino acid starvation in bacteria leads to coupled cessation of protein synthesis and stable RNA synthesis, a process known as the "stringent response" that is accompanied by accumulation of poly P. Poly P accumulation is mediated by alarmone guanosine 5′-diphosphate 3′-diphosphate synthesis, which ultimately inhibits an exopolyphosphatase, an enzyme that degrades poly P (40). Together with the cessation of nucleic acid synthesis and continued assimilation of P_i from the medium, this results in large accumulations of poly P. Although guanosine 5′-diphosphate 3′-diphosphate has been found in plants (41), it is not known whether it is present in early branched eukaryotes. In support of the notion that TOR kinases could be involved in poly P metabolism, it has been shown that poly P stimulates mammalian TOR kinase activity *in vitro* and most likely *in vivo* (10). It is important to mention that knockdown of *T. brucei* TOR2 kinase does not cause poly P accumulation, although a substantial growth inhibition and an increase in cell size occur (5), indicating that poly P accumulation is specific for TbTOR-like 1 knockdown.

Poly P has been shown to be essential for adaptation to various stresses and for survival of bacteria in the stationary phase (43–45). Similar studies have been reported in eukaryotic cells, such as yeast (46), fungi (47), and algae (48). It has long been recognized that the poly P content is low during rapid growth and increases under conditions of nutritional imbalance unfavorable for growth in different organisms from bacteria to yeast (49). Knockdown of TbTOR-like 1 might have a phenotype similar to that of nutritional imbalance.

Studies of TOR signaling in yeast, *Drosophila*, and mammals have demonstrated that TOR kinases participate directly in cellular growth and size control. In these organisms ablation of TOR leads to a decrease in cell size by several mechanisms (4, 51). One mechanism appears to involve a balance between signaling pathways interfering with cell cycle control and growth (52). In the case of TbTOR-like 1, knocked down PCF are larger than control cells, similar to what is observed for TbTOR2 but opposite to the TbTOR1 knockdown phenotype (5). In addition, when mammalian TORC1 and *T. brucei* TOR1 expression are reduced, cells arrest in the G_1 phase of the cell cycle (5, 53),

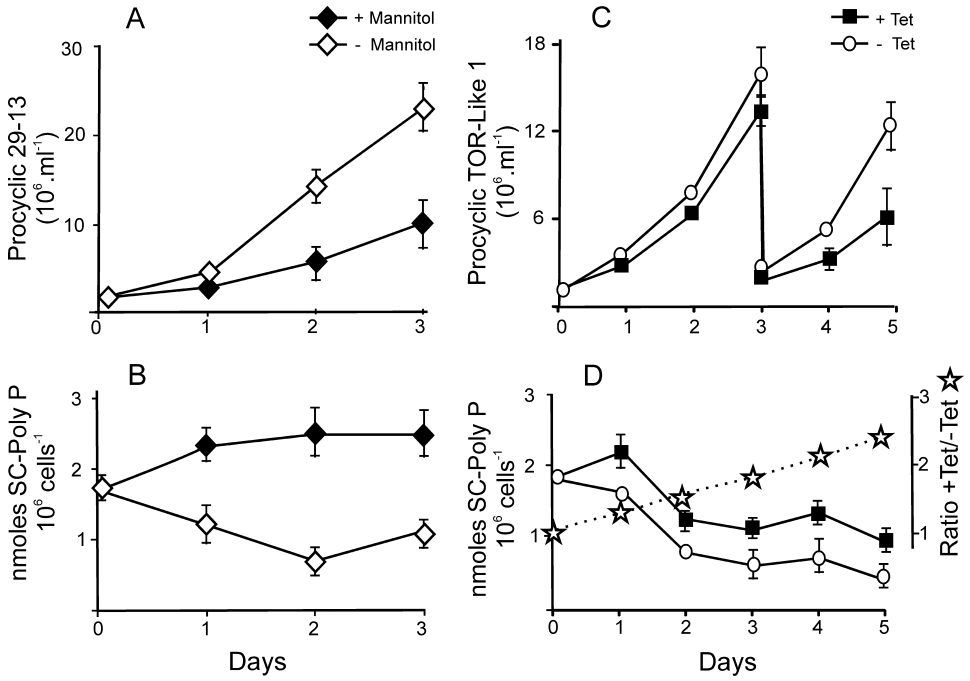

FIGURE 9. **Hyperosmotic medium causes a similar increase of poly P as TbTOR-like 1 ablation.** *T. brucei* PCF 29-13 (*A* and *B*) and PCF containing the p2T7-177 TbTOR-like 1 vector (*C* and *D*) were grown in regular medium (*open symbols*) or medium with 0.3 M mannitol for PCF 29-13 or with 1 μg/ml tetracycline for PCF TbTOR-like 1 (*closed symbols*). The number of parasites was counted daily, and the amount of short chain poly P was measured in triplicate experiments. The values are the means ± S.D. For all values, $p < 0.05$. The *stars* indicate the ratios of poly P levels between cells incubated in the presence and absence of tetracycline.

whereas TbTOR-like 1-depleted cells accumulate at the S/G_2 phase. The increased amount of zoids (0N1K) found here was also observed for TbTOR-like 2 knocked down cells (53). However, in this case cells also accumulate in the G_1 phase as found for TbTOR1 RNAi. In contrast, TbTOR2 knocked down cells accumulate in G_1 with the formation of multinucleated and multiflagellated cells (5). Different from TbTOR-like 1, TbTOR2 RNAi resulted in multinucleated cells with an enlarged flagellar pocket without the appearance of dense acidocalcisomes. TbTOR1 RNAi causes autophagy events without the appearance of dense acidocalcisome granules. All of these findings indicate that TOR kinases of *T. brucei* act through different mechanisms and might have different substrates and/or activators, probably affecting growth, proliferation, and cell cycle control at different points as proposed earlier (54, 55).

Decrease of TbTORs expression also differently affects PCF and BSF, which may reflect differences observed in cell cycle control between these stages of the parasite (56). For example, PCF form multinucleated cells, zoids, and other abnormal cell types when TbTOR 1 expression is reduced (53), whereas in BSF these effects are not observed (5). When TbTOR-like 2 expression is reduced, the cells accumulate at S/G_2 in PCF, generating zoids and multinucleated cells, whereas no effect is evident in BSF when the same protein is ablated (53). In the present case PCF delay in S/G_2 is more evident than in BSF (data not shown). The mechanism by which TbTOR-like 1 and other TbTOR affect *T. brucei* cell cycle requires further investigation. Nevertheless, one possibility is that a delay in the S/G_2 phase might occur by inhibition of *de novo* nucleotide synthesis because of a decrease of free phosphate resulting from the accumulation of poly P. Alternatively, the delay in the cell cycle could be directed by a similar mechanism found in the fission yeast, in which TOR 1 affects the mitogen-activated protein kinase (MAPK) control of cell cycle progression (52). In this sense, it is relevant that the osmotic stress in *Schizosaccharomyces pombe* cross-talks with TOR signaling (57). A similar cross-talk might occur for TbTOR-like 1.

One unique characteristic of TbTOR-like 1 is the presence of the PDZ domain. This domain is involved in the scaffolding and assembly of multi-protein complexes at various subcellular sites, which suggests their participation in several aspects of cellular physiology such as receptor or channel clustering, cell junction formation, and intracellular signaling events (58). Our results unequivocally demonstrate that TbTOR-like 1 has a cytosolic distribution in dispersed granules because RNAi knockdown abolishes immunofluorescence labeling. This result is compatible with the formation of multiprotein complexes between the kinase and other unidentified proteins, and this is supported by the fact that upon gel filtration of soluble extracts, TbTOR-like 1 eluted with sizes corresponding to proteins from 200 to 650 kDa (data not shown). Moreover, TbTOR-like 1 does not colocalize with any of the markers used to label specific organelles, suggesting that it might form a new type of structure. Perhaps the presence of the PDZ domain is involved in this different type of cytosolic complex. In contrast, TbTOR 1 is nuclear, and TbTOR 2, which lacks the PDZ domain, seems to be associated with the endoplasmic reticulum or the mitochondrial membrane (5), as found for yeast and mammalian TORC complexes (42, 59–62). It is important to mention that the identification of other partners of TbTOR-like 1 and its substrates, determination of whether TbTOR-like 1 affects translation, and demonstration of kinase activity will be necessary to characterize this protein.

A relevant finding of this work is that hyperosmotic stress changes momentously the localization of TbTOR-like 1. Immunofluorescence labeling revealed that it becomes clustered near the parasite surface, different from glycosomes, endoplasmic reticulum, and stress granules. Some cellular reorganization of the single trypanosome mitochondrion is noticed, suggesting that it could participate in the same signaling pathway. Because PDZ domains are found in several types of dynamic protein-protein interactions (50), it is tempting to speculate that changing protein localization during osmotic stress is important for TbTOR-like 1 function. The next step would be to identify proteins that interact with the PDZ domain of TbTOR-like 1.

Taken together, the present results characterize a new type of TOR-like enzyme that might have an important adaptive role in *T. brucei*. Because we could not access all parasite stages found in the insect forms or during transition between insect and mammalian host, it is possible that TbTOR-like 1 would have other specific roles in addition to being able to detect nutritional variations. In these different situations, *T. brucei* must be able to detect changes in osmolarity to modify its cell structure and metabolism. Much evidence indicates that acidocalcisomes are effectors of these modifications through the balance of poly P and PP_i complexed with cations (9), but much less is known about how cell signals promote osmotic compensations. TbTOR-like 1 could be this link.

Acknowledgments—We thank Claudio Rogerio de Oliveira, Luana Umeda, and Mariana Leão de Lima for experimental help support and Beatriz A. Castilho and Nilson Zanchin for helpful suggestions.

REFERENCES

1. Gull, K. (2001) *Int. J. Parasitol.* **31,** 443–452
2. Vieira, L. L. (1998) *Biochim. Biophys. Acta* **1376,** 221–241
3. Wullschleger, S., Loewith, R., and Hall, M. N. (2006) *Cell* **124,** 471–484
4. Jacinto, E., and Hall, M. N. (2003) *Nat. Rev. Mol. Cell Biol.* **4,** 117–126
5. Barquilla, A., Crespo, J. L., and Navarro, M. (2008) *Proc. Natl. Acad. Sci. U.S.A.* **105,** 14579–14584
6. Loewith, R., Jacinto, E., Wullschleger, S., Lorberg, A., Crespo, J. L., Bonenfant, D., Oppliger, W., Jenoe, P., and Hall, M. N. (2002) *Mol. Cell* **10,** 457–468
7. Kornau, H. C., Seeburg, P. H., and Kennedy, M. B. (1997) *Curr. Opin. Neurobiol.* **7,** 368–373
8. Kornberg, A., Rao, N. N., and Ault-Riché, D. (1999) *Annu. Rev. Biochem.* **68,** 89–125
9. Docampo, R., de Souza, W., Miranda, K., Rohloff, P., and Moreno, S. N. (2005) *Nat. Rev. Microbiol.* **3,** 251–261
10. Wang, L., Fraley, C. D., Faridi, J., Kornberg, A., and Roth, R. A. (2003) *Proc. Natl. Acad. Sci. U.S.A.* **100,** 11249–11254
11. Ruiz, F. A., Rodrigues, C. O., and Docampo, R. (2001) *J. Biol. Chem.* **276,** 26114–26121
12. Vercesi, A. E., Moreno, S. N., and Docampo, R. (1994) *Biochem. J.* **304,** 227–233
13. Docampo, R., Scott, D. A., Vercesi, A. E., and Moreno, S. N. (1995) *Biochem. J.* **310,** 1005–1012
14. Rohloff, P., Rodrigues, C. O., and Docampo, R. (2003) *Mol. Biochem. Parasitol.* **126,** 219–230
15. Scott, D. A., de Souza, W., Benchimol, M., Zhong, L., Lu, H. G., Moreno, S. N., and Docampo, R. (1998) *J. Biol. Chem.* **273,** 22151–22158
16. Scott, D. A., Docampo, R., Dvorak, J. A., Shi, S., and Leapman, R. D. (1997) *J. Biol. Chem.* **272,** 28020–28029
17. Scott, D. A., and Docampo, R. (2000) *J. Biol. Chem.* **275,** 24215–24221
18. Wirtz, E., and Clayton, C. (1995) *Science* **268,** 1179–1183
19. Wirtz, E., Leal, S., Ochatt, C., and Cross, G. A. (1999) *Mol. Biochem. Parasitol.* **99,** 89–101
20. Wickstead, B., Ersfeld, K., and Gull, K. (2002) *Mol. Biochem. Parasitol.* **125,** 211–216
21. Clayton, C. E., Estévez, A. M., Hartmann, C., Alibu, V. P., Field, M., and Horn, D. (2005) *Methods Mol. Biol.* **309,** 39–60
22. Abuin, G., Freitas-Junior, L. H. G., Colli, W., Alves, M. J., and Schenkman, S. (1999) *J. Biol. Chem.* **274,** 13041–13047
23. Church, G. M., and Gilbert, W. (1984) *Proc. Natl. Acad. Sci. U.S.A.* **81,** 1991–1995
24. Wang, Z., Morris, J. C., Drew, M. E., and Englund, P. T. (2000) *J. Biol. Chem.* **275,** 40174–40179
25. McDowell, M. A., Ransom, D. M., and Bangs, J. D. (1998) *Biochem. J.* **335,** 681–689
26. Bangs, J. D., Uyetake, L., Brickman, M. J., Balber, A. E., and Boothroyd, J. C. (1993) *J. Cell Sci.* **105,** 1101–1113
27. Holetz, F. B., Correa, A., Avila, A. R., Nakamura, C. V., Krieger, M. A., and Goldenberg, S. (2007) *Biochem. Biophys. Res. Commun.* **356,** 1062–1067
28. Lemercier, G., Dutoya, S., Luo, S., Ruiz, F. A., Rodrigues, C. O., Baltz, T., Docampo, R., and Bakalara, N. (2002) *J. Biol. Chem.* **277,** 37369–37376
29. Schöneck, R., Billaut-Mulot, O., Numrich, P., Ouaissi, M. A., and Krauth-Siegel, R. L. (1997) *Eur. J. Biochem.* **243,** 739–747
30. Hammarton, T. C., Clark, J., Douglas, F., Boshart, M., and Mottram, J. C. (2003) *J. Biol. Chem.* **278,** 22877–22886
31. Kocic, I., Hirano, Y., and Hiraoka, M. (2001) *Cardiovasc. Res.* **51,** 59–70
32. Miranda, K., Docampo, R., Grillo, O., and de Souza, W. (2004) *Protist* **155,** 395–405
33. Fang, J., Rohloff, P., Miranda, K., and Docampo, R. (2007) *Biochem. J.* **407,** 161–170
34. Ruiz, F. A., Luo, S., Moreno, S. N., and Docampo, R. (2004) *Microsc. Microanal.* **10,** 563–567
35. Andrade, M. A., and Bork, P. (1995) *Nat. Genet.* **11,** 115–116
36. Bosotti, R., Isacchi, A., and Sonnhammer, E. L. (2000) *Trends Biochem. Sci.* **25,** 225–227
37. Choi, J., Chen, J., Schreiber, S. L., and Clardy, J. (1996) *Science* **273,** 239–242
38. Ponting, C. P., Phillips, C., Davies, K. E., and Blake, D. J. (1997) *Bioessays* **19,** 469–479
39. Rohloff, P., Montalvetti, A., and Docampo, R. (2004) *J. Biol. Chem.* **279,** 52270–52281
40. Brown, M. R., and Kornberg, A. (2004) *Proc. Natl. Acad. Sci. U.S.A.* **101,** 16085–16087
41. Takahashi, K., Kasai, K., and Ochi, K. (2004) *Proc. Natl. Acad. Sci. U.S.A.* **101,** 4320–4324
42. Kim, J. E., and Chen, J. (2000) *Proc. Natl. Acad. Sci. U.S.A.* **97,** 14340–14345
43. Ault-Riché, D., Fraley, C. D., Tzeng, C. M., and Kornberg, A. (1998) *J. Bacteriol.* **180,** 1841–1847
44. Rao, N. N., Liu, S., and Kornberg, A. (1998) *J. Bacteriol.* **180,** 2186–2193
45. Rao, N. N., and Kornberg, A. (1996) *J. Bacteriol.* **178,** 1394–1400
46. Castro, C. D., Meehan, A. J., Koretsky, A. P., and Domach, M. M. (1995) *Appl. Environ. Microbiol.* **61,** 4448–4453
47. Yang, Y. C., Bastos, M., and Chen, K. Y. (1993) *Biochim. Biophys. Acta* **1179,** 141–147
48. Pick, U., and Weiss, M. (1991) *Plant Physiol.* **97,** 1234–1240
49. Harold, F. M., and Harold, R. L. (1965) *J. Bacteriol.* **89,** 1262–1270
50. Feng, W., and Zhang, M. (2009) *Nat. Rev. Neurosci.* **10,** 87–99
51. Wang, X., and Proud, C. G. (2009) *Trends Cell Biol.* **19,** 260–267
52. Petersen, J. (2009) *Biochem. Soc. Trans.* **37,** 273–277
53. Monnerat, S., Clucas, C., Brown, E., Mottram, J. C., and Hammarton, T. C. (2009) *BMC Res. Notes* **2,** 46
54. Barquilla, A., and Navarro, M. (2009) *Autophagy* **5,** 256–258
55. Barquilla, A., and Navarro, M. (2009) *Cell Cycle* **8,** 697–699
56. Tu, X., and Wang, C. C. (2004) *J. Biol. Chem.* **279,** 20519–20528
57. López-Avilés, S., Grande, M., González, M., Helgesen, A. L., Alemany, V., Sanchez-Piris, M., Bachs, O., Millar, J. B., and Aligue, R. (2005) *Mol. Cell* **17,** 49–59
58. Charest, A., Lane, K., McMahon, K., and Housman, D. E. (2001) *J. Biol. Chem.* **276,** 29456–29465
59. Díaz-Troya, S., Pérez-Pérez, M. E., Florencio, F. J., and Crespo, J. L. (2008) *Autophagy* **4,** 851–865
60. Wedaman, K. P., Reinke, A., Anderson, S., Yates, J., 3rd, McCaffery, J. M., and Powers, T. (2003) *Mol. Biol. Cell* **14,** 1204–1220
61. Desai, B. N., Myers, B. R., and Schreiber, S. L. (2002) *Proc. Natl. Acad. Sci. U.S.A.* **99,** 4319–4324
62. Drenan, R. M., Liu, X., Bertram, P. G., and Zheng, X. F. (2004) *J. Biol. Chem.* **279,** 772–778